# Fractional topological excitations and quantum phase transition in a bilayer two-dimensional electron gas adjacent to a superconductor film

Ningning Hao,[1,2] Wei Zhang,[1] Zhigang Wang,[1] Yupeng Wang,[2] and Ping Zhang[1,3,*]
[1]*Institute of Applied Physics and Computational Mathematics, P.O. Box 8009, Beijing 100088, People's Republic of China*
[2]*Institute of Physics, Chinese Academy of Sciences, Beijing 100080, People's Republic of China*
[3]*Center for Applied Physics and Technology, Peking University, Beijing 100871, People's Republic of China*
(Received 16 September 2009; revised manuscript received 28 January 2010; published 1 March 2010)

We study a bilayer two-dimension-electron-gas (2DEG) adjacent to a type-II superconductor thin film with a pinned vortex lattice. We find that with increasing interlayer tunneling, the system of half-filling presents three phases: gapped phase-I (topological insulator), gapless critical phase-II (metal), and gapped phase-III (band insulator). The total Hall conductance for phase-I/III is $2/0\ e^2/h$, and has nonquantized values in phase-II. The excitation (response to topological defect, a local vortex defect) in these three phases shows different behaviors due to the topological property of the system, including fractional charge $e/2$ for each layer in phase-I. While in the case of quarter-filling, the system undergoes a quantum phase transition from metallic phase to topological insulator phase.

DOI: 10.1103/PhysRevB.81.125301 PACS number(s): 73.43.−f, 71.10.Pm, 74.25.Uv

## I. INTRODUCTION

Topological excitation and fractional charge have attracted considerable attention for decades. Jackiw and Rebbi first found topological excitation with fractionalized charge in one-dimensional (1D) system of a Dirac fermion field coupling with a topologically nontrivial Bose field.[1] Su *et al.* provided a nice intuitive picture for charge $e/2$ soliton in polyacetylene chain.[2] Goldstone and Wilczek discussed the possibility of irrational charge in 1+1D systems.[3] The two-dimensional (2D) fractional quantum Hall (QH) system with strong correlation and time-reversal symmetry (TRS) broken, first studied by Tsui *et al.*,[4] supports elementary excitations of the many-body ground state with fractional charge and fractional statistics.[5] Recently, Hou *et al.*[6] have studied a model of graphenelike structures with a vortex configuration in the Kekulé modulations of the hopping amplitudes. They have found a fractional charge $e/2$ bonded to the vortex without breaking TRS. Similar phenomenon was found in a model of 2D square lattice with the analogical modulations of the hopping amplitudes.[7] These results indicate that the TRS and strong correlation are not the necessary conditions for charge fractionalization in 2D.

Weeks *et al.*[8] proposed another experimentally accessible 2D weakly interacting system of two-dimensional electron gas (2DEG) in the integer QH state adjacent to a film of type-II superconductor supplying the quantization of flux in units of $\frac{1}{2}\Phi_0$ ($\Phi_0=h/e$). They found the excitations with fractional charge and anyonic statistics which can be described by a wave function composed by a set of filled one-particle states. Moreover, the system could be fabricated in the laboratory.[9]

As is known, bilayer system may show new interesting features compared with those of the corresponding monolayer system, for example, the bilayer QH system versus the monolayer QH system. In this paper, we study the bilayer 2DEG adjacent to a film of type-II superconductor. The feasibility of the similar system with monolayer 2DEG was argued by Seradjeh *et al.* in detail.[9] Our studies show that the system undergoes quantum phase transitions from gapped phase-I/topological insulator (TI) to gapless critical phase-II/metal, then to gapped phase-III/band insulator (BI) with increasing interlayer tunneling at half-filling (here, half-filling means electronic filling factor=number of electrons/number of sites. It also implies one electron per magnetic cell; note that a magnetic cell is twice of a monolayer crystalline cell. Sometimes it is also helpful to use the magnetic filling factor=number of electrons/number of flux quanta. Thus half electronic filling is the same as magnetic filling factor 2. Similarly, quarter electronic filling is the same as magnetic filling factor 1). These quantum phase transitions are not related to any symmetry breaking. The difference between TI phase and BI phase is that the energy spectrum of the edged system in the former has gapless topological edge state. Furthermore, we find that the three phases have different Hall conductances and excitations as response to the flux defect, i.e., an extra or missing $\frac{1}{2}\Phi_0$ flux in the vortex lattices shows different charge density profiles. The excitation of the TI phase has charge $e/2$ for each layer. While at quarter-filling case, there are one gapless metallic phase and one gapped TI phase.

## II. LATTICE MODEL AND ENERGY SPECTRUM

The tight-binding Hamiltonian for independent electrons in the presence of square vortex lattice is given by

$$H_{latt}=-\sum_{\langle i,j\rangle\alpha} t_{ij}e^{i\theta_{ij\alpha}}c_{i\alpha}^{+}c_{j\alpha}-\sum_{\langle\langle i,j\rangle\rangle\alpha} t_{1ij}e^{i\varphi_{ij\alpha}}c_{i\alpha}^{+}c_{j\alpha}-t_2\sum_{i,\alpha\neq\beta} c_{i\alpha}^{+}c_{i\beta}, \quad (1)$$

where $\alpha(\beta)=1,2$ refers to different layers, $\langle i,j\rangle(\langle\langle i,j\rangle\rangle)$ represents the nearest-neighbor (next-nearest-neighbor) sites, $t_{ij}$ ($t_{1ij}$) is hopping amplitude between nearest-neighbor (next-nearest-neighbor) sites in the same layer, and $t_2$ is the interlayer tunneling amplitude. In this work, for simplicity, we assume that $t_{ij}=t$ and $t_{1ij}=t_1$. We have neglected the electron-

 

electron interaction and also assumed that the spins of all electrons are polarized along the field. $c_{i\alpha}$ annihilates an electron at site $\mathbf{r}_i$ in layer $\alpha$. In the following we set the lattice constant $a=1$, $t=1$, $t_1/t=\gamma_1$, and $t_2/t=\gamma_2$.

The effect of magnetic field is included through the Peierls phase factors

$$\theta_{ij\alpha}=\frac{2\pi}{\Phi_0}\int_{\mathbf{r}_i}^{\mathbf{r}_j}_{\langle i,j\rangle\alpha}\mathbf{A}_\alpha\cdot d\mathbf{r},\quad \varphi_{ij\alpha}=\frac{2\pi}{\Phi_0}\int_{\mathbf{r}_i}^{\mathbf{r}_j}_{\langle\langle i,j\rangle\rangle}\mathbf{A}_\alpha\cdot d\mathbf{r},$$

with $\mathbf{A}_\alpha=\frac{\Phi_0}{2}(0,x)$ the vector potential in Landau gauge so that each plaquette in layer $\alpha$ is uniformly threaded by a flux $\frac{1}{2}\Phi_0$. The magnetic unit cell in layer $\alpha$ includes two sites $(l,m)\alpha$ and $(l+1,m)\alpha$ denoted by $A\alpha$ and $B\alpha$. In bilayer system, the wave function is of the form of spinor field $\psi(\mathbf{r})=(c_{B1}(\mathbf{r}_{l+1m}),c_{A1}(\mathbf{r}_{lm}),c_{B2}(\mathbf{r}_{l+1m}),c_{A2}(\mathbf{r}_{lm}),)^T$. The bilayer Hamiltonian can be diagonalized in the momentum space, with the reduced Brillouin zone $BZ=\{\mathbf{k}:|k_x|\le\pi/2,|k_y|\le\pi\}$, as $H_{latt}=\Sigma_{\mathbf{k}}\psi_{\mathbf{k}}^{+}\tilde{H}_{\mathbf{k}}\psi_{\mathbf{k}}$, where $\psi_{\mathbf{k}}=(c_{B1}(\mathbf{k}),c_{A1}(\mathbf{k}),c_{B2}(\mathbf{k}),c_{A2}(\mathbf{k}))^T$. Furthermore, after a rotation of the spinor field, $\varphi_{\mathbf{k}}=S^{+}\psi_{\mathbf{k}}$, with $S=\exp(i\pi I\otimes\sigma_x/4)\exp(i\pi I\otimes\sigma_z/4)\exp(i\pi I\otimes\sigma_x/2)$, with $\sigma_{x,y,z}$ the Pauli matrices, the Hamiltonian $H_{\mathbf{k}}$ has a simplified form

$$\begin{aligned}H_{\mathbf{k}}&=S^{+}\tilde{H}S\\&=I\otimes(2\cos k_y\sigma_x+2\cos k_x\sigma_y+4\gamma_1\sin k_x\sin k_y\sigma_z)\\&\quad+\gamma_2\sigma_x\otimes I.\end{aligned}\tag{2}$$

We define the operator $G\equiv i\sigma_y\otimes\sigma_y$ and it is easy to see that $GH^{*}G=H$, $G^2=-1$. As a consequence, for each eigenstate $\varphi_E$ with eigenvalue $E$, there is a corresponding eigenstate $G\varphi_E^{*}$ with eigenvalue $-E$. The energy bands of $H_{\mathbf{k}}$ are given explicitly by

$$E_1(\mathbf{k})=\gamma_2+\varepsilon(\mathbf{k}),E_2(\mathbf{k})=\gamma_2-\varepsilon(\mathbf{k}),$$

$$E_3(\mathbf{k})=-\gamma_2+\varepsilon(\mathbf{k}),E_4(\mathbf{k})=-\gamma_2-\varepsilon(\mathbf{k}),\tag{3}$$

where $\varepsilon(\mathbf{k})=2\sqrt{\cos^2 k_x+\cos^2 k_y+4\gamma_1^2\sin^2 k_x\sin^2 k_y}$. The energy bands are symmetric about zero energy. The bands are sketched in Fig. 1 for different values of interlayer tunneling $\gamma_2$. There are four branches of the curves corresponding to Eq. (3). For the half-filling case, when the maximum of $E_2(\mathbf{k})$ is lager than the maximum of $E_4(\mathbf{k})$ and smaller than the minimum of $E_3(\mathbf{k})(0<\gamma_2<4\gamma_1)$, the bands $E_2(\mathbf{k})$ and $E_3(\mathbf{k})$ are separated with a gap $\Delta=8\gamma_1-2\gamma_2$. The system is in a TI phase due to the existence of gapless edge states (with topological winding numbers) for the edged sample, or nontrivial Chern number as seen later. When the maximum of $E_2(\mathbf{k})$ is lager than the minimum of $E_3(\mathbf{k})$ and the minimum of $E_2(\mathbf{k})$ is smaller than the maximum of $E_3(\mathbf{k})(4\gamma_1<\gamma_2<2\sqrt{2})$,[11] the bands $E_2(\mathbf{k})$ and $E_3(\mathbf{k})$ mix each other, leading to disappearance of the gap. When the minimum of $E_2(\mathbf{k})$ is larger than the maximum of $E_3(\mathbf{k})(\gamma_2>2\sqrt{2})$, the gap reappear, showing the behavior of a usual BI. For the quarter-filling case, when the minimum of $E_2(\mathbf{k})$ is smaller than the maximum of $E_4(\mathbf{k})(\gamma_2<\sqrt{2}-2\gamma_1)$, the bands $E_2$ and $E_4$ mix each other leading to gapless metallic phase; when the minimum of $E_2(\mathbf{k})$ is larger than the maximum of $E_4(\mathbf{k})\gamma_2>\sqrt{2}-2\gamma_1$, the system is always in the TI phase with a gap $\Delta=2(\gamma_2-(\sqrt{2}-2\gamma_1))$.

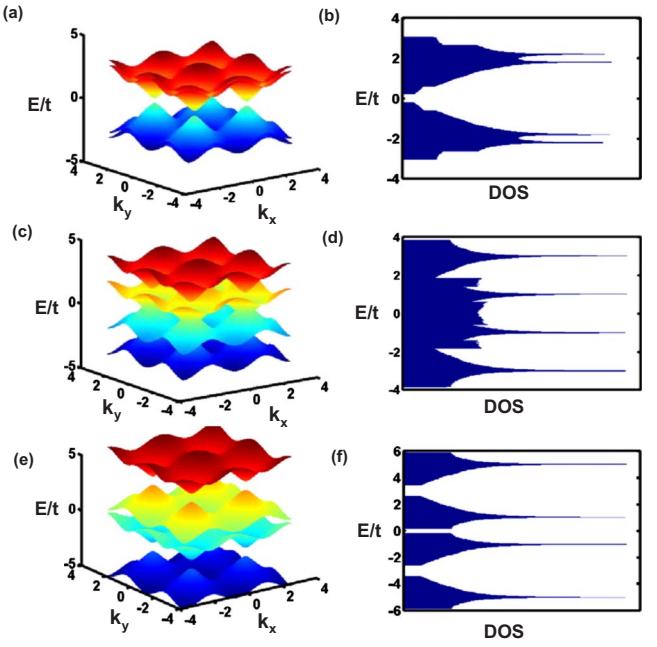


FIG. 1. (Color online) The energy band structures of the lattice Hamiltonian (1) with different $\gamma_2$: (a) $\gamma_2=0.2$, (c) $\gamma_2=1.0$, (e) $\gamma_2=3.0$. $\gamma_1=0.1$. The corresponding densities of the states in arbitrary unit are shown in (b), (d), and (f).

We can see the different topological properties of the TI and BI phases in the samples with edges. We calculate the energy bands for the sample with edges in $y$ direction under different parameters shown in Fig. 2. In TI phases, we can find the bands of edge states crossing the gap at $ka=\pi/2$, while no bands cross the gap in BI phase. The TI phases can be characterized by the Chern number in the bulk theory and by winding number in the edge state theory. The Chern number and winding number are equivalent.

## III. QUANTUM PHASE TRANSITIONS

We look at the quantum phase transitions with changing of the interlayer tunneling further from other point of view. First, we rewrite the system's Hamiltonian with $\gamma_2$ as the control parameter,

$$H_{\mathbf{k}}(\gamma_2)=H_{\mathbf{k}}^{(0)}+\gamma_2 H_{\mathbf{k}}^{(1)}\tag{4}$$

where $H_{\mathbf{k}}^{(0)}=I\otimes(2\cos k_y\sigma_x+2\cos k_x\sigma_y+4\gamma_1\sin k_x\sin k_y\sigma_z)$ and $H_{\mathbf{k}}^{(1)}=\sigma_x\otimes I$. Note that $[H_{\mathbf{k}}^{(0)},H_{\mathbf{k}}^{(1)}]=0$. Thus quantum phase transition may appear as a few lowest energy levels cross and the properties of ground-state change dramatically.[12] One may also find possible quantum phase transitions by calculating the ground-state fidelity, defined as the overlap between $\Psi_0(\gamma_2)$ and $\Psi_0(\gamma_2+\delta)$,[13]

$$F(\gamma_2,\delta)=|\langle\Psi_0(\gamma_2+\delta)|\Psi_0(\gamma_2)\rangle|,\tag{5}$$

where $\delta$ is a small quantity, and the many-body ground-state wave functions of the system $\Psi_0$ can be constructed with the

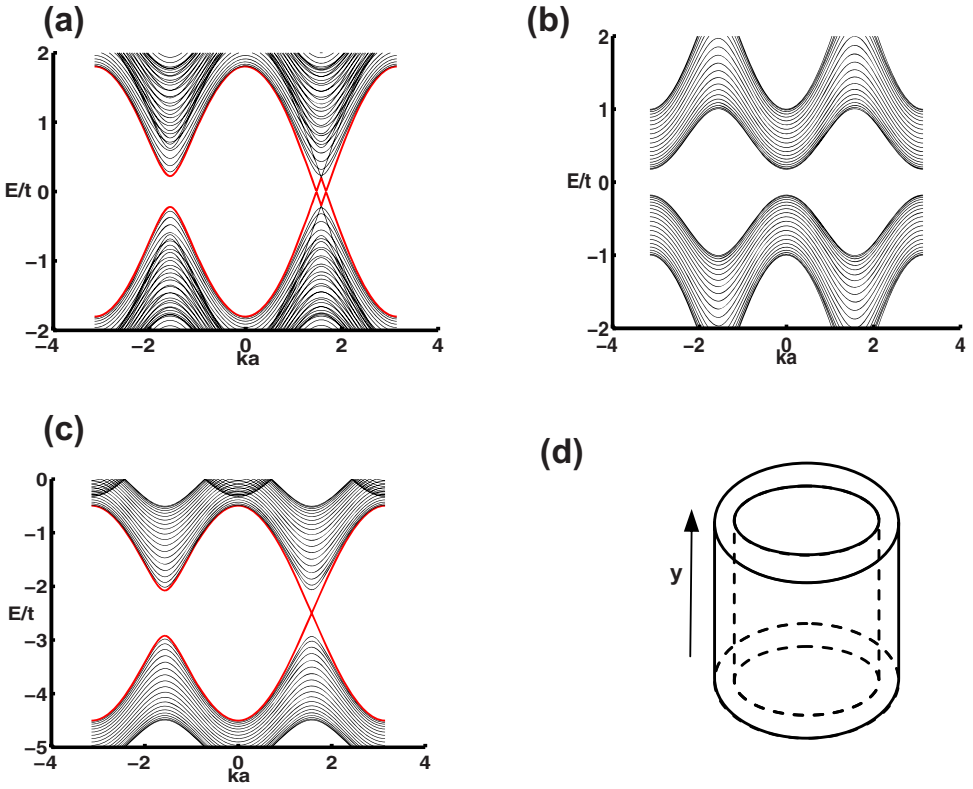


FIG. 2. (Color online) Energy bands for the one-dimensional strip. (a) TI phase with $\gamma_2=0.2$ for half-filling case; (b) BI phase with $\gamma_2=3$ for half-filling case; (c) TI phase with $\gamma_2=2.5$ for quarter-filling case. In all cases, we use the cylindrical geometry shown in (d) with 40 sites in y direction and $\gamma_1=0.1$.

one-particle wave functions through the Slater determinant. In the numerical calculation of the fidelity, we have used 40 000 basis and $\delta=0.005$. The fidelity as a function of $\gamma_2$ is shown in Fig. 3. We see that it is always constant and equal to unity in the two regions of $0<\gamma_2<4\gamma_1$ and $\gamma_2>2\sqrt{2}$ for the half-filling case, indicating that each region corresponds to a specific phase. The fact that the fidelity is equal to zero in the region $4\gamma_1<\gamma_2<2\sqrt{2}$ tells us the system is in the critical phase in this region, which is consistent with the absence of gap and lack of characteristic length scale in phase-II. Similarly, in the case of quarter-filling ($\nu=1/4$), there are only two phases separated by the critical point $\gamma_{2,c}=\sqrt{2}-2\gamma_1$. These results are consistent with what we have found based on the analysis of the energy spectrums and can be described by the energy-level crossing.[12]

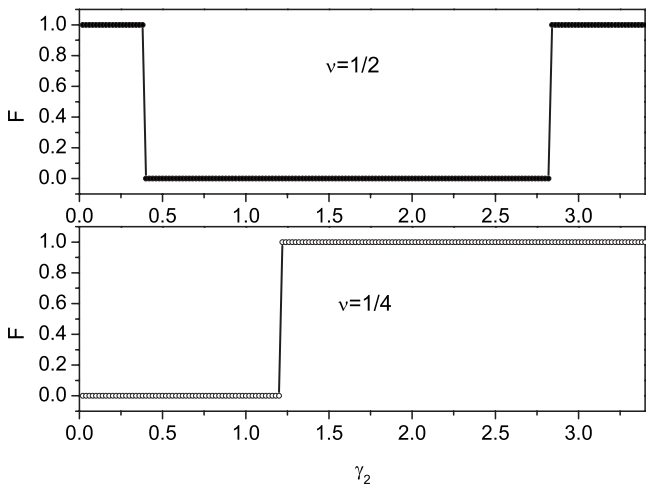


FIG. 3. The fidelity versus interlayer coupling $\gamma_2$. $\gamma_1=0.1$.

## IV. TOPOLOGICAL EXCITATIONS AND FRACTIONAL CHARGES

We first calculate the total Hall conductance for the bilayer system based on the Kubo formula $\sigma_H=\frac{e^2}{h}C$ with $C=\frac{1}{2\pi}\Sigma_n\int^{E_F}d^2k\hat{z}\cdot[\nabla_{\mathbf{k}}\times A_n(\mathbf{k})]$, where the upper limit means that the integration is over all occupied states below the Fermi energy $E_F$. Here $A_n(\mathbf{k})=i\langle\psi_n(\mathbf{k})|\nabla_{\mathbf{k}}\psi_n(\mathbf{k})\rangle$ is the Berry phase connection for $n$th band with wave function $\psi_n(\mathbf{k})$. When the Fermi level is in the gap, one has the well-known (Thouless, Kohmoto, Nightingale, and Nijs) TKNN formula[10] $C=\Sigma_n C_n$, where $C_n=\frac{1}{2\pi}\int_{BZ}d^2k\hat{z}\cdot[\nabla_{\mathbf{k}}\times A_n(\mathbf{k})]$ is the Chern number. The results for the Hall conductance is shown in Fig. 4, which reflect the different properties of the three (two) phases for the case of half (quarter) filling. It is clearly seen that in the half-filling case, the total Hall conductance is 2/0 (in unit of $e^2/h$) in the phase-I/III, and is not quantized in the gapless phase-II; in the quarter-filling case, the total Hall conductance is 1 in the gapped phase-II, and is not quantized in the gapless phase-I. It is seen that the total Hall conductance in the TI phase is related to the magnetic filling factor for both half-filling and quarter-filling cases.

The topological excitation appears as the response to the perturbation added to the system. Here the perturbation is in a form of a flux defect $\eta\Phi_0(\eta=\pm\frac{1}{2})$ to the vortex lattice as discussed in Ref. 8. The vector potential in each layer has the following modulation $\delta\mathbf{A}_\alpha=\frac{\eta\Phi_0}{2\pi r^2}(\mathbf{r}\times\hat{z})$. Correspondingly, the modulation to Peierls factors is

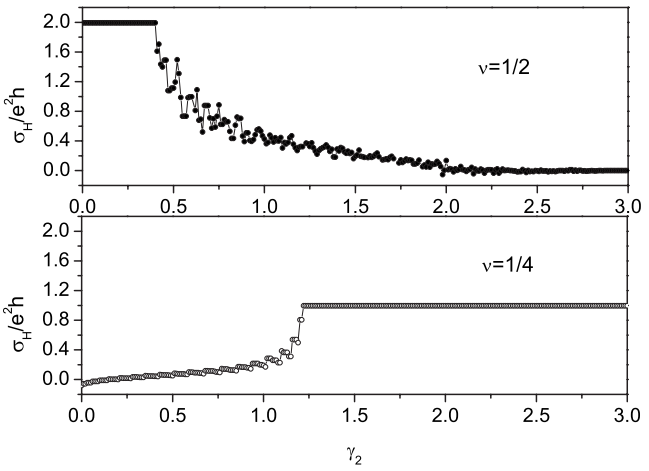


FIG. 4. The total Hall conductance versus interlayer coupling $\gamma_2$. $\gamma_1=0.1$.

$$\delta\theta_{ij\alpha}=\frac{2\pi}{\Phi_0}\int_{\langle i,j\rangle\alpha}^{\mathbf{r}_j}_{\mathbf{r}_i}\delta\mathbf{A}_\alpha\cdot d\mathbf{r}=\eta\int_{\langle i,j\rangle\alpha}^{\mathbf{r}_j}_{\mathbf{r}_i}d\theta,$$

$$\delta\varphi_{ij\alpha}=\frac{2\pi}{\Phi_0}\int_{\langle\langle i,j\rangle\rangle\alpha}^{\mathbf{r}_j}_{\mathbf{r}_i}\delta\mathbf{A}_\alpha\cdot d\mathbf{r}=\eta\int_{\langle\langle i,j\rangle\rangle\alpha}^{\mathbf{r}_j}_{\mathbf{r}_i}d\theta. \quad (6)$$

In a stringy gauge, the Peierls factors can be specified as $\delta\theta_{ij}=\pi(\delta\varphi_{ij}=\pi)$ if the string, originating from the defect and ending at a boundary, cuts the $i$-$j$ bond, and zero otherwise. These extra Peierls factors have the properties $\oint\delta\theta_{ij}=\pi$ mod $2\pi$ ($\oint\delta\varphi_{ij}=\pi$ mod $2\pi$) for closed loop containing the defect. They look like a vortex profile. These topologically nontrivial Peierls factors have profound effects on the behavior of the excitation.

Let us look at the basic properties of the excitation, as the response of the system to the flux defect, in the three phases for the case of half-filling. Since phase-I and phase-III are gapped, thus are incompressible, the charge for each layer due to the presence of the flux defect is $\delta Q=\eta\sigma_H e/2$, as argued in Ref. 8. Combining with above results of the conductance, we have $\delta Q=e/2$ (for $\eta=1/2$) in phase-I and $\delta Q=0$ in phase-III. To confirm this result and gain more understanding of the properties of the three phases, we perform a numerical calculation based on exact diagonalizations of lattice Hamiltonian. We have applied this method to the systems of sizes up to $48\times48$ at different values of interlayer tunneling $\gamma_2$ and obtained the charge density profile (per layer) as presented in Fig. 5. The two layers have the same results since the defects in each layer are superposable along the magnetic field direction. By integration of the density profile, we get the charge for each layer $\delta Q=e/2$ (0) for the gapped phase-I (III), agreeing with the above arguments based on the incompressibility and Hall conductance. The situation is quite different for the gapless phase II. The charge profile is nonlocal and there is no well-defined localized charge due to the lack of characteristic length scale in the gapless critical phase-II. This is unlike the gapped

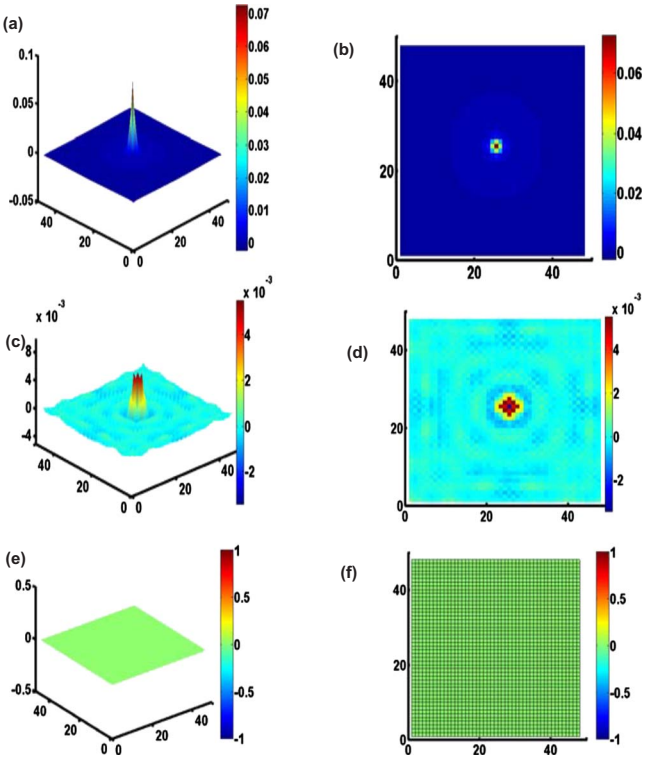


FIG. 5. (Color online) The charge densities of the excitation for different $\gamma_2$ at half-filling: (a) $\gamma_2=0.2$, (c) $\gamma_2=1.0$, (e) $\gamma_2=3.0$, in a $48\times48$ lattice system with periodic boundary condition. (b), (d), (f) are the corresponding plan forms. In all cases, we have subtracted the background charge density which is uniformly equal to 0.5 on each site of the lattice at the half-filling case. $\gamma_1=0.1$.

phase-I, where the presence of localized charge is due to the nontrivial Peierls phase profile and characteristic length scale determined by the gap.

Having seen the essential difference between the gapped and gapless phases, we now explore more difference between the two gapped phases. From the different values of Hall conductance, we have already seen that the difference between phase-I and phase-III is due to their different topological properties. In fact, explicit calculation of edged systems in Fig. 2 shows the existence of gapless edge states in phase-I, while they are absent in phase-III. More understanding can be obtained by studying their low energy behavior. In phase-I, the low energy excitation can be described by the system Hamiltonian expanded around the points $\mathbf{K}\equiv(\frac{\pi}{2},\pm\frac{\pi}{2})$, $H_{\mathbf{K}}=I\otimes(2k_y\sigma_x+2k_x\sigma_y+4\gamma_1\sigma_z)+\gamma_2\sigma_x\otimes I$ with energy spectrum $E_{\mathbf{k}}=\pm\gamma_2\pm2\sqrt{k^2+4\gamma_1^2}$ and $\mathbf{k}$ the momentum relative to $\mathbf{K}$. In this case, the Hamiltonian is of the Dirac type with first-order differential operators. When the system is in the phase-III, the low energy excitation can be described by the system Hamiltonian expanded around the points $\overline{\mathbf{K}}=(0,\pi)$ [or (0,0)], $H_{\overline{\mathbf{K}}}=I\otimes[2(1-k_y^2/2)\sigma_x+2(1-k_x^2/2)\sigma_y]+\gamma_2\sigma_x\otimes I$ with energy spectrum $E_{\overline{\mathbf{K}}}=\pm\gamma_2\pm\sqrt{2}(2-k^2/2)$. Clearly, unlike phase-I, the Hamiltonian for phase-III is a Schrödinger type of second-order differential operators. Also, since the $\gamma_1$ term disappears in $H_{\overline{\mathbf{K}}}$, the low energy physics in phase III is thus insensitive to the vortex profile and looks more like ordinary

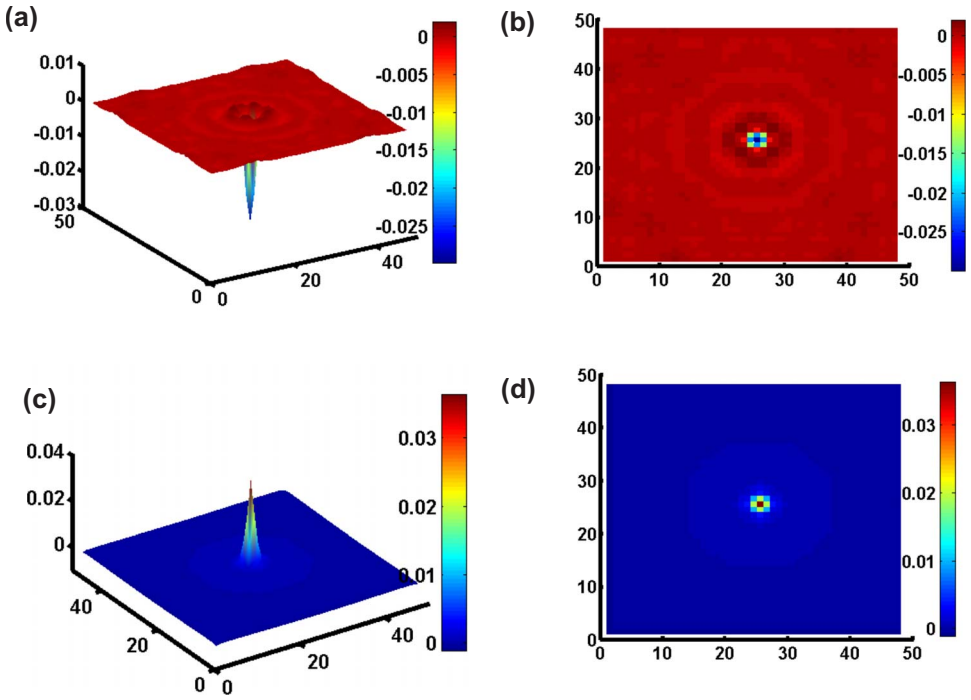


FIG. 6. (Color online) The charge densities of the excitation for different $\gamma_2$ at quarter-filling: (a) $\gamma_2=0.8$, (c) $\gamma_2=2.5$, in a $48\times48$ lattice system with periodic boundary condition. (b), (d) are the corresponding plan forms. In all cases, we have subtracted the background charge density which is uniformly equal to 0.25 on each site of the lattice at the quarter-filling case. $\gamma_1=0.1$.

BI. These discussions reveal the essential difference between TI (phase-I) and BI (phase-III).

Now we briefly discuss the case with quarter-filling. In this case, as shown in last section, there are two phases: gapless critical phase-I and gapped phase-II. In phase-I the Hall conductance is not quantized (as shown in Fig. 4) and there is no well-defined localized charge. While in phase-II, the Hall conductance is quantized at $1e^2/h$. With the same numerical method as the half-filling case, the charge density profile (per layer) is presented in Fig. 6 for the systems of sizes up to $48\times48$ at different values of interlayer tunneling $\gamma_2$. Our numerical calculations show that the integral over charge density for two layers is $e/2$ (see Fig. 6), which is consistent with the estimation $\delta Q=\eta\sigma_H e=e/2$. However, unlike the half-filling TI phase, in the quarter-filling TI phase the charge for each layer is not robust against perturbations such as on-site energy, disorder etc.

The results of a single layer[8,9] may help people understanding partial results of the present bilayer system. For half-filling, when the interlayer coupling is weak, each layer looks like a single layer in the inter quantum hall regime and each layer may be in a TI phase with fractional charge $e/2$. One important issue is the robustness of the topological nature of TI ensures the stability of the bilayer system for weak perturbation from interlayer coupling and leads to a phase transition from TI phase to metallic phase at *finite* interlayer coupling, rather than zero interlayer coupling. For quarter-filling with strong interlayer coupling, the magnetic filling factor is 1 and one has the total fractional charge for bilayer $e/2$ as seen before.

Before ending our discussion, we address briefly the accessibility of the parameters. There are three important length scales in our bilayer system: magnetic length $l_B$, the penetration length of the type-II superconductor $\lambda_L$, and the interlayer distance $d$. $l_B=\sqrt{\frac{\hbar}{eB}}\simeq\frac{25.6}{\sqrt{B(\text{Tesla})}}$ nm, so $l_B$ has several nanometers when the magnetic field of $\sim10$ T. The pinned Abrikosov lattice constant $a$ has the same scale of $l_B$, which makes it easier to realize $\Phi_0/2$ per plaquette than the natural solid with lattice constant of $\sim0.1$ nm, requiring the magnetic field in order of $10^4$ T. As discussed in the Ref. 8, the vortices are well separated and the defects are well localized from the estimation of $\lambda_L$. The interlayer distance $d$ can be tuned in experiment and is related to the key parameter $t_2$ (or $\gamma_2$) in our bilayer system. Unlike other natural systems such as bilayer graphene with $\gamma_2\ll1$,[14] $\gamma_2$ can have values in a very large regime by tuning the width of the wells (which form 2DEG) in the growth direction, as well as the width and height of the barrier between the wells.

## V. CONCLUSION

We have investigated the bilayer 2DEG adjacent to type-II superconductor thin film. We find that the system undergoes quantum phase transitions between several different phases through modulating the interlayer tunneling: gapped phase/topological insulator, gapless critical phase/metal, and gapped phase/band insulator. Depending on different (topological) properties of each phase, the system shows different Hall conductance, accompanying with appearance/disappearance of topological excitation with fractional charge of $e/2$.

## ACKNOWLEDGMENTS

This work was partially supported by NSFC under Grants No. 10604010, No. 10874020, and No. 10574150, by CAEP under Grant No. 2008B0102004, and by the National Basic Research Program of China (973 Program) under Grants No. 2009CB929103 and No. 2006CB921300.

*Corresponding author; zhang_ping@iapcm.ac.cn

[1] R. Jackiw and C. Rebbi, Phys. Rev. D **13**, 3398 (1976).
[2] W. P. Su, J. R. Schrieffer, and A. J. Heeger, Phys. Rev. Lett. **42**, 1698 (1979).
[3] J. Goldstone and F. Wilczek, Phys. Rev. Lett. **47**, 986 (1981).
[4] D. C. Tsui, H. L. Stormer, and A. C. Gossard, Phys. Rev. Lett. **48**, 1559 (1982).
[5] R. B. Laughlin, Phys. Rev. Lett. **50**, 1395 (1983).
[6] C.-Y. Hou, C. Chamon, and C. Mudry, Phys. Rev. Lett. **98**, 186809 (2007).
[7] B. Seradjeh, C. Weeks, and M. Franz, Phys. Rev. B **77**, 033104 (2008).
[8] C. Weeks, G. Rosenberg, B. Seradjeh, and M. Franz, Nat. Phys. **3**, 796 (2007).
[9] G. Rosenberg, B. Seradjeh, C. Weeks, and M. Franz, Phys. Rev. B **79**, 205102 (2009).
[10] D. J. Thouless, M. Kohmoto, M. P. Nightingale, and M. den Nijs, Phys. Rev. Lett. **49**, 405 (1982).
[11] For most situation, the hopping amplitude between nearest-neighbor sites is much larger than that between next-nearest-neighbor sites, i.e., $\gamma_1 \ll 1$ and $4\gamma_1 < 2\sqrt{2}$.
[12] S. Sachdev, *Quantum Phase Transitions* (Cambridge University Press, Cambridge, England, 1999).
[13] P. Zanardi and N. Paunkovic, Phys. Rev. E **74**, 031123 (2006).
[14] R. Dillenschneider and J. H. Han, Phys. Rev. B **78**, 045401 (2008); J. Nilsson, A. H. Castro Neto, F. Guinea, and N. M. R. Peres, *ibid.* **78**, 045405 (2008).